International Journal of Innovative
Computing, Information and Control
Volume **15**, Number **6**, December **2019**

 ISSN 1349-4198
pp. **2259–2273**

OPTIMAL PI$^\lambda$D$^\mu$ CONTROLLER DESIGN BASED ON SPIRITUAL SEARCH FOR WIND TURBINE SYSTEMS

Deacha Puangdownreong

Department of Electrical Engineering
Southeast Asia University
19/1 Petchkasem Road, Nongkhangphlu, Nonghkaem, Bangkok 10160, Thailand
deachap@sau.ac.th

Received February 2019; revised June 2019

Abstract. *This paper proposes the optimal PI$^\lambda$D$^\mu$ controller (or fractional-order PID) design for wind turbine systems by using the spiritual search (SS), one of the newest and most efficient hybrid metaheuristic optimization searching algorithms. Based on the modern optimization, the SS is conducted in this work to search for appropriate values of five parameters of the PI$^\lambda$D$^\mu$ controller to achieve control designing purposes including command-tracking and load-regulating. The proposed SS-based design approach is demonstrated to design the optimal PI$^\lambda$D$^\mu$ controllers for a drive train model and a pitch control model of the wind turbine systems. With the SS-based design, results obtained by the PI$^\lambda$D$^\mu$ controllers will be compared with those obtained by the conventional PI and PID controllers. As results, it was found that the SS can optimize PI, PID and PI$^\lambda$D$^\mu$ controllers corresponding to the given design constraints, specifications and search spaces. By comparison, the PID controller provides better responses than the PI. However, the PI$^\lambda$D$^\mu$ controller outperforms PI and PID in both command-tracking and load-regulating purposes.*

Keywords: PI$^\lambda$D$^\mu$ controller, Spiritual search, Wind turbine system, Metaheuristic optimization

1. **Introduction.** Nowadays, numerous renewable energy technologies have been studied and developed for solving the world energy crisis problems. Among those renewable energy technologies, wind power is the world's fastest growing source [1-4]. In wind power systems, there are commonly two main kinds of wind generators, i.e., vertical-axis and horizontal-axis. They can be used to generate large amounts of electricity in wind farms which can be installed on both onshore and offshore. In order to achieve a stable power output once the wind speed is above the rated wind speed, the pitch control is applied by adjusting the pitch angle of the wind turbine blades. Normally, wind turbine system will be automatically operated under the feedback control loop with the proportional-integral (PI) [5,6], the proportional-integral-derivative (PID) controller [7-10], fuzzy-PID controller [11,12] and expert control system [13].

In 1994, the PI$^\lambda$D$^\mu$ (or fractional-order PID) controller was firstly proposed by Podlubny [14,15]. As an extended version of the conventional PID controller, the PI$^\lambda$D$^\mu$ controller possesses five tuning parameters. Superiority of the PI$^\lambda$D$^\mu$ to the conventional PID controller has been proved [14,15]. Following the literature, the PI$^\lambda$D$^\mu$ controller has been successfully conducted in many control applications, for instance, process control [16], automatic voltage regulator [17], DC motor control [18], power electronic control [19], inverted pendulum control [20] and gun control system [21]. Several design and tuning

DOI: 10.24507/ijicic.15.06.2259

methods for the PI$^{\lambda}$D$^{\mu}$ controller have been consecutively launched, for example, rule-based methods [22,23] and analytical methods [24,25]. Review and tutorial articles of the PI$^{\lambda}$D$^{\mu}$ controller providing the state-of-the-art and its backgrounds have been completely reported [26,27].

Control synthesis has been changed from the conventional paradigm to the new framework based on modern optimization by using metaheuristics as an optimizer [28,29]. By literature reviews, some well-known metaheuristic algorithms have been applied for designing optimal PI/PID controllers of wind turbine systems, for example, genetic algorithm (GA) [30,31] and particle warm optimization (PSO) [32,33]. Among those metaheuristics, the spiritual search (SS) is one of the newest and most efficient metaheuristic optimization searching techniques [34]. The SS is firstly proposed in 2018 and conceptualized by the spiritual concentration according to the Buddhist principles. As the hybrid metaheuristic algorithm, single solution-based (trajectory-based) and population-based approaches are combined in the SS algorithm to balance the advantages of exploration and exploitation properties. For preliminary study [34], it was found that the SS can provide optimal solutions of several standard benchmarking functions with the highest percentage of success rate for finding global solutions and the shortest search-time consumed once compared with tabu search (TS) and cuckoo search (CS). Moreover, the SS was successfully applied to model identification, PID and PIDA controllers design [34,35]. In addition, the applications of the SS to designing an optimal PI$^{\lambda}$D$^{\mu}$ controller for wind turbine systems do not appear in literature.

In this paper, an optimal PI$^{\lambda}$D$^{\mu}$ controller design for a drive train and a pitch control of the wind turbine systems based on the SS is proposed. With the proposed SS-based design approach, results obtained by the PI$^{\lambda}$D$^{\mu}$ controllers will be compared with those obtained by the PI and PID controllers. This paper is arranged as follows. After an introduction is provided in Section 1, the PI$^{\lambda}$D$^{\mu}$ controller based on fractional calculus is briefly described in Section 2. Modeling of a drive train and a pitch control of the wind turbine systems is given in Section 3. The SS-based PI$^{\lambda}$D$^{\mu}$ controller design problem is formulated in Section 4. Results and discussion are illustrated in Section 5. Finally, conclusions are followed in Section 6.

2. PI$^{\lambda}$D$^{\mu}$ Controller.

A generalization of integration and differentiation can be represented by the non-integer order fundamental operator ${}_aD_t^{\alpha}$, where a and t are the limits of the operator. The continuous integro-differential operator is defined as expressed in (1), where $\alpha \in \Re$ stands for the order of operation.

$$ {}_aD_t^{\alpha} = \begin{cases} \dfrac{d^{\alpha}}{dt^{\alpha}} & \Re(\alpha) > 0 \\ 1 & \Re(\alpha) = 0 \\ \displaystyle\int_a^t (d\tau)^{-\alpha} & \Re(\alpha) < 0 \end{cases} \tag{1} $$

The classical PID controller model is expressed in (2) and (3), where K_p is proportional gain, K_i is integral gain, K_d is derivative gain, $u(t)$ is the control signal (regarded as an output variable) and $e(t)$ is the error signal (regarded as an input variable). It consists of three elements, i.e., proportional (P) element, integral (I) element and derivative (D) element, respectively. In the feedback control loop, the classical PID controller can be represented by the block diagram in Figure 1.

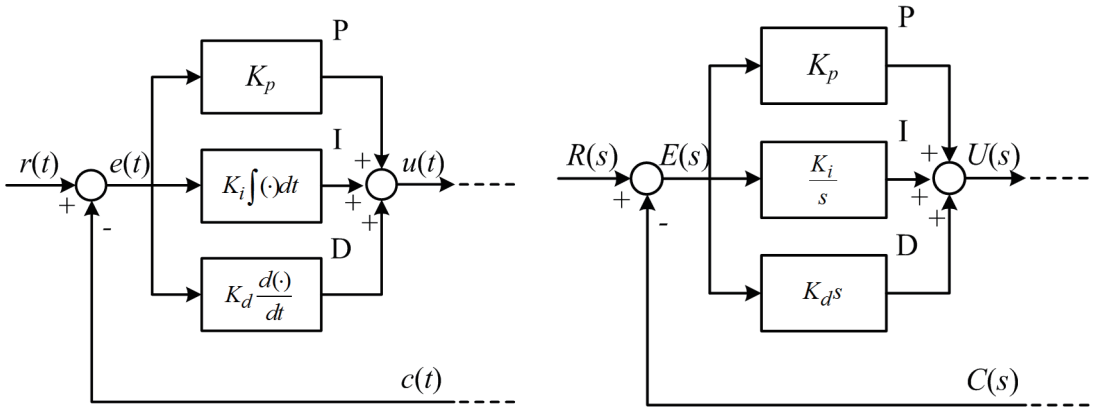

(a) Time-domain (b) s-domain

FIGURE 1. The classical PID controller: (a) PID controller in time-domain and (b) PID controller in s-domain

$$\left.\begin{aligned} u(t) &= K_p e(t) + K_i \int e(t)dt + K_d \frac{de(t)}{dt} \\ &= K_p e(t) + K_i D_t^{-1} e(t) + K_d D_t e(t) \end{aligned}\right\} \tag{2}$$

$$G_c(s)|_{PID} = K_p + \frac{K_i}{s} + K_d s \tag{3}$$

The PI$^{\lambda}$D$^{\mu}$ controller is an extended version of the conventional PID controller. It can be regarded as the general controller for all PID family members. The PI$^{\lambda}$D$^{\mu}$ controller possesses five tuning parameters, i.e., K_p, K_i, K_d, integral order (λ) and derivative order (μ). The generalized transfer function of the PI$^{\lambda}$D$^{\mu}$ controller is given by the differential equation as stated in (4), while λ and $\mu \geq 0$, and by the Laplace transform as stated in (5).

$$u(t) = K_p e(t) + K_i D_t^{-\lambda} e(t) + K_d D_t^{\mu} e(t) \tag{4}$$

$$G_c(s)|_{PI^{\lambda}D^{\mu}} = K_p + \frac{K_i}{s^{\lambda}} + K_d s^{\mu} \tag{5}$$

Referring to (5), λ is the fractional order of the integral element, while μ is the fractional order of the derivative element. The step responses of the PI$^{\lambda}$D$^{\mu}$ controller are shown in Figure 2. Once $\lambda = 1$ and $\mu = 1$, the PI$^{\lambda}$D$^{\mu}$ is the conventional PID. The step response of this case is depicted in Figure 2(a). It was found that the portion a depends on K_p. The greater the value of K_p, the greater the portion a. It was known that K_p will decrease the rise time and the steady-state error of the system response. The portion b depends on K_d. The more the value of K_d, the more the portion b. It was known that K_d will decrease the settling time and the oscillation of the system response. The slope d depends on K_i. The greater the value of K_i, the greater the slope d. It was also known that K_i will eliminate the steady-state error of the system response.

From Figure 2(b) and Figure 2(c), μ is fixed and λ is varied. It was shown that λ will affect the portion e. This implies that λ will reinforce K_i to eliminate the steady-state error of the system response rapidly. From Figure 2(d) and Figure 2(e), λ is fixed, while μ is varied. It was found that μ will affect the portion c. This implies that μ will reinforce K_d to decrease the settling time and the oscillation of the system response effectively.

Relationship between the conventional PID and the PI$^{\lambda}$D$^{\mu}$ can be represented by a graphical way as visualized in Figure 3 [26,27]. In general, the range of fractional orders (λ and μ) is varied from 0 to 2. However, in most research works, the range of λ and

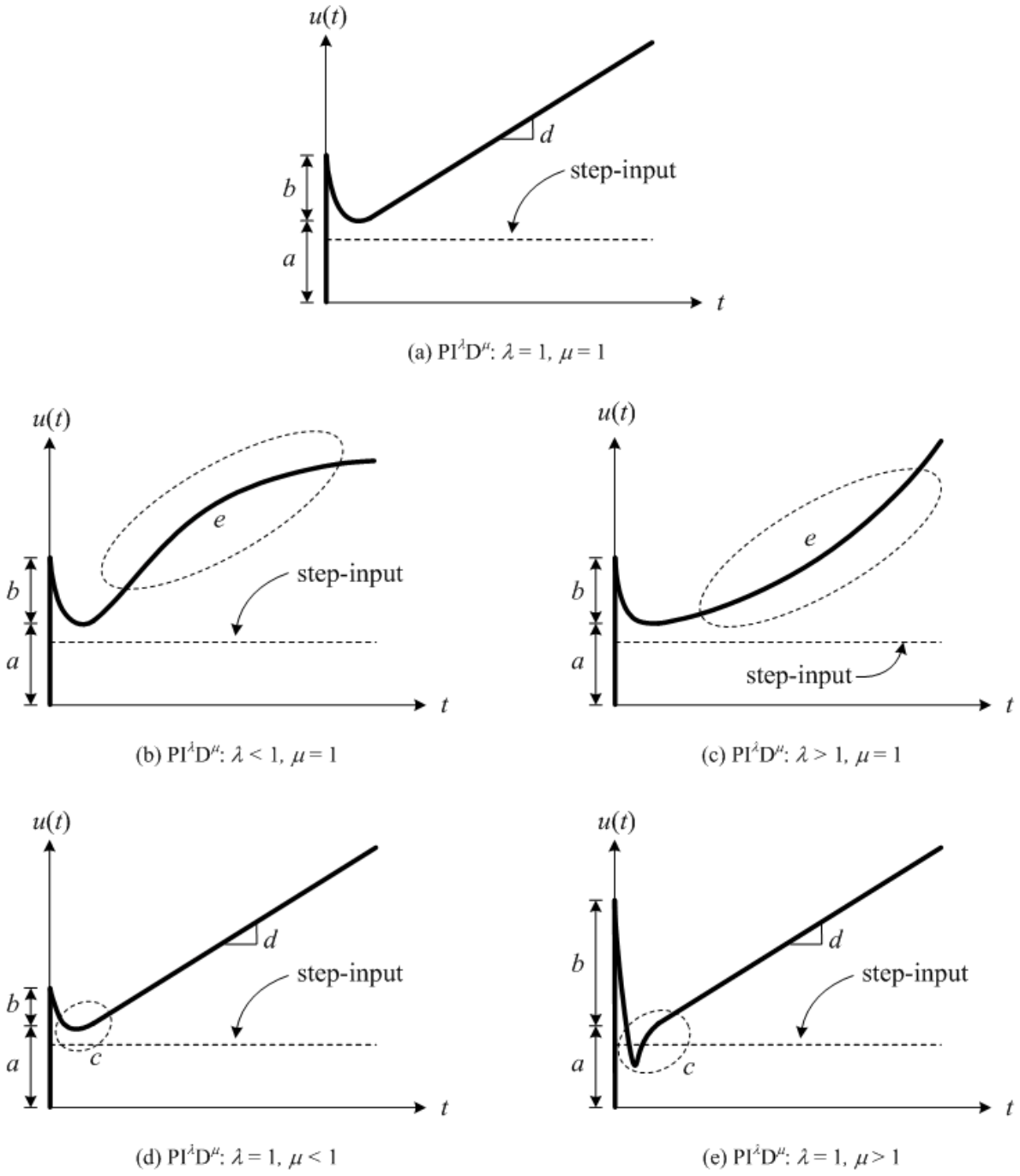

FIGURE 2. Step responses of PI$^{\lambda}$D$^{\mu}$ controller: (a) $\lambda = 1$ and $\mu = 1$, (b) $\lambda < 1$ and $\mu = 1$, (c) $\lambda > 1$ and $\mu = 1$, (d) $\lambda = 1$ and $\mu < 1$ and (e) $\lambda = 1$ and $\mu > 1$

μ is varied from 0 to 1. Referring to Figure 3, if $\lambda = \mu = 1$, it is the conventional PID controller.

With its five tuning parameters, designing an optimal PI$^{\lambda}$D$^{\mu}$ controller is a challenging work especially for higher-order systems. In this paper, an optimal PI$^{\lambda}$D$^{\mu}$ controller design for higher-order wind turbine systems based on the SS is proposed.

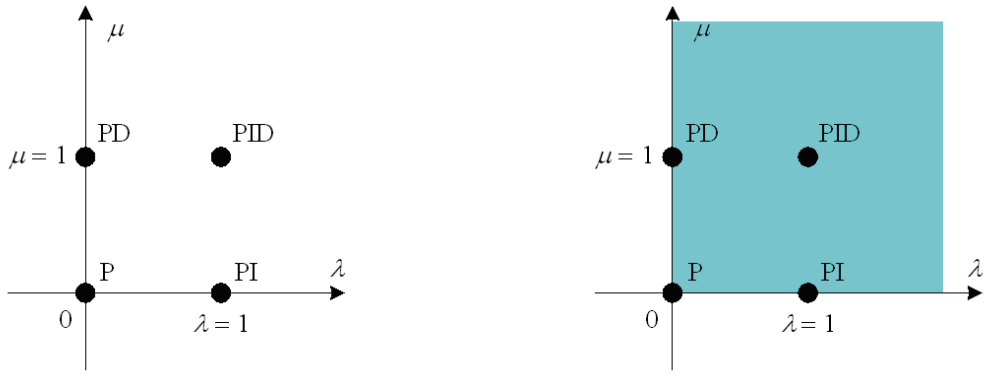

(a) PID (b) PI$^{\lambda}$D$^{\mu}$

FIGURE 3. PID and PI$^{\lambda}$D$^{\mu}$ from points to plane: (a) integer-order and (b) fractional-order

3. **Wind Turbine System Models.** Based on the aerodynamic lift principle, wind turbines can be divided according to the orientation of the axis of rotation on the horizontal-axis wind turbine (HAWT) and vertical-axis wind turbine (VAWT) which can be installed on the land or sea as shown in Figure 4 [1-4]. However, the horizontal-axis or propeller-type wind turbines are most commonly used for wind farms, community wind projects, and small wind applications. This is because the HAWT generator can provide higher wind energy conversion efficiency and access to stronger wind due to high tower. Thus, the HAWT generator will be focused and conducted in this work. The simplified structures of a wind turbine consist of large blades, a powerful rotor, a strong hub and a gearbox. The wind turbine system must be capable of operating over a wide range of wind speeds. Therefore, a double-feed induction generator (DFIG) was commonly used [1-4].

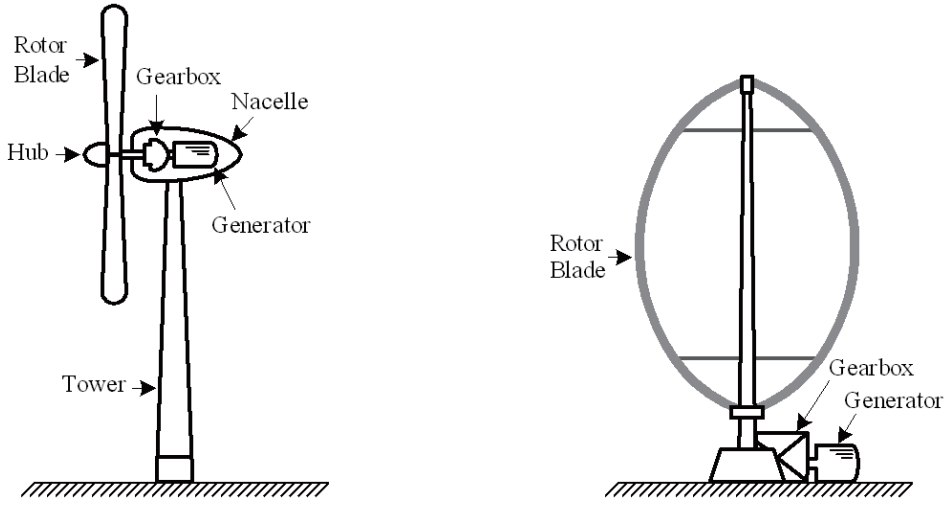

(a) HAWT (b) VAWT

FIGURE 4. Wind turbine configurations: (a) horizontal-axis wind turbine (HAWT) and (b) vertical-axis wind turbine (VAWT)

3.1. **Drive train model.** The drive train consists of the wind turbine rotor, low-speed shaft, gearbox, high-speed shaft, and the DFIG. Basically, the model of a wind turbine drive train is a three-mass rotational mechanical model with flexible shafts on both wind turbine and generator sides. Such the three masses correspond to a large mass of the

wind turbine rotor, a mass for the gearbox wheels, and a mass for generator, respectively. However, the moments of inertia for the shafts and gearbox wheels can be lumped or neglected because they are very small once compared with the moment of inertia of the wind turbine or generator. Thus, the model can be reduced to a two-mass rotational mechanical model as shown in Figure 5, where $T_A(t)$ is the aerodynamic torque applied from wind turbine speed (velocity of rotor), J_T is the lumped moment of inertia of rotor and low-speed shaft, $\omega_T(t)$ is the turbine-side speed, K_{lss} is the low-speed shaft stiffness, D_{lss} is the low-speed shaft damping factor, $\omega_{gT}(t)$ is the turbine-side gearbox speed, N is the gearbox ratio, $\omega_{gG}(t)$ is the generator-side gearbox speed, K_{hss} is the high-speed shaft stiffness, D_{hss} is the high-speed shaft damping factor, $\omega_G(t)$ is the generator-side speed, J_G is the lumped moment of inertia of generator and high-speed shaft and $T_e(t)$ is the electromagnetic torque generated by DFIG.

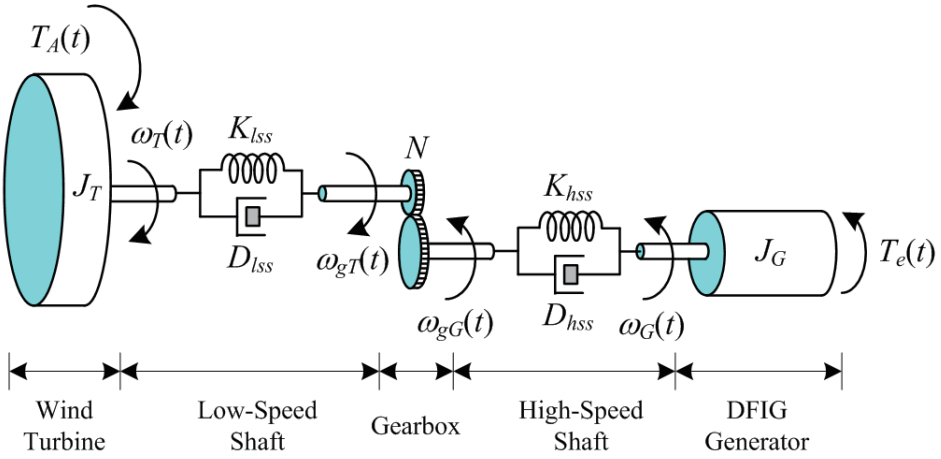

FIGURE 5. Wind turbine drive train

In this work, the wind turbine of 330-kW in [36] is conducted. The s-domain transfer function model, $G_{p1}(s)$, of the wind turbine drive train is given as expressed in (6) [33,36].

$$G_{p1}(s) = \frac{2.28 \times 10^{19} s}{9.941 \times 10^{12} s^5 + 4.971 \times 10^{14} s^4 + 1.024 \times 10^{17} s^3 + 7.534 \times 10^{17} s^2 + 5.685 \times 10^{18} s} \tag{6}$$

3.2. **Pitch control model.** The pitch-driven system was operated by using hydraulic pressure. Although the system is typically used in large power systems, it included a time delay for the wind turbine generation system. In this work, the pitch control model of the wind turbine with 275-kW generator in [37,38] is conducted. The s-domain transfer function model, $G_{p2}(s)$, of the pitch control system of the wind turbine is given as stated in (7) [33,37,38].

$$G_{p2}(s) = \left(\frac{-0.6219 s^2 - 8.7165 s - 2911}{s^4 + 5.018 s^3 + 691.3 s^2 + 1949 s + 1.15 \times 10^5} \right) e^{-0.25 s} \tag{7}$$

From the drive train and the pitch control models in (6) and (7), they will be used as the plants controlled by the PI$^\lambda$D$^\mu$ controller optimized by the SS as detailed in next section.

4. **SS-Based PI$^\lambda$D$^\mu$ Controller Design Problem Formulation.** In this section, the SS algorithm is briefly described, the PI$^\lambda$D$^\mu$ control loop is illustrated, and the SS-based PI$^\lambda$D$^\mu$ control design problem is then formulated.

4.1. **SS algorithm.** The spiritual search (SS) was firstly proposed in 2018 by Puangdownreong [34]. As hybrid metaheuristic optimization algorithm conceptualized by the spiritual concentration called "Samatha-Kammatthana" according to the Buddhist principles [39,40], the SS algorithm possesses single solution-based (trajectory-based) and population-based approaches to balance the advantages of exploration and exploitation properties. The SS algorithm was formulated based on three following rules [34]:

Rule-1 Once *Citta* travels to explore various sense-objects, it is regarded as the population-based metaheuristics having exploration property by using random process with unlimited distribution. In this case, Lévy distribution with an infinite variance and an infinite mean is conducted.

Rule-2 When *Citta* meets concentration state with only one particular sense-object, it is regarded as the single solution-based metaheuristics having exploitation property by using random process with normal distribution denoted by $N(\mu, \sigma^2)$, where μ is the mean and $\sigma > 0$ is the standard deviation. For the standard normal distribution, $\mu = 0$ and $\sigma = 1$ are denoted by $N(0, 1)$.

Rule-3 Switching between travelling *Citta* and concentrating *Citta* can be defined by the switching probability, ρ.

From Rule-1, the mathematical relation for updating a new solution is expressed in (8)-(13) [34], where $\boldsymbol{x}^{t+1}$ is the updated solution, $\boldsymbol{x}^t$ is the previous solution, L is a random number with Lévy distribution, Γ is standard gamma function, s is a step size, u and v are a random number with normal distribution, and σ_u and σ_v are the standard deviation.

$$\boldsymbol{x}_i^{t+1} = \boldsymbol{x}_i^t + L\left(\boldsymbol{x}_j^t - \boldsymbol{x}^*\right) \tag{8}$$

$$L \approx \frac{\alpha\beta\Gamma(\beta)\sin\left(\pi\beta/2\right)}{\pi|s|^{1+\beta}}, \quad s \to \infty, \quad 0 < \beta \leq 2 \tag{9}$$

$$\Gamma(z) = \int_0^{\infty} t^{z-1}e^{-t}dt \tag{10}$$

$$s = \frac{u}{|v|^{1/\beta}} \tag{11}$$

$$u \approx N\left(0, \sigma_u^2\right), \quad v \approx N\left(0, \sigma_v^2\right) \tag{12}$$

$$\sigma_u = \left\{\frac{\Gamma(1+\beta)\sin(\pi\beta/2)}{\Gamma[(1+\beta)/2]\beta 2^{(\beta-1)/2}}\right\}^{1/\beta}, \quad \sigma_v = 1 \tag{13}$$

Regarding to Rule-2, the mathematical relation for updating a new solution $\boldsymbol{x}^{t+1}$ is expressed in (14)-(15) [34], where ε is a random number with normal distribution.

$$\boldsymbol{x}_i^{t+1} = \boldsymbol{x}_i^t + \varepsilon\left(\boldsymbol{x}_j^t - \boldsymbol{x}^*\right) \tag{14}$$

$$\varepsilon = \frac{1}{\sigma\sqrt{2\pi}}e^{-\left\{\frac{(\boldsymbol{x}-\mu)^2}{2\sigma^2}\right\}}, \quad -\infty < \boldsymbol{x} < \infty \tag{15}$$

Referring to Rule-3, the switching probability ρ is fixed at particular value and γ is randomly generated in each moment (iteration). If $\gamma > \rho$, the Rule-1 is activated. Otherwise, Rule-2 is invoked. The SS algorithm can be summarized by pseudo code as shown in Figure 6.

Referring to Figure 6 representing the SS algorithm, the objective function $f(\boldsymbol{x})$, numbers of population of sens-objects (solutions) n and switching probability ρ are firstly initialized. Also, the initial best solution has to be evaluated via the given objective function. In the iteration process, the SS algorithm will check the difference between γ and ρ. If $\gamma > \rho$, the Rule-1 (population-based) is activated by using the expressions in (8)-(13)

- Objective function $f(\boldsymbol{x})$, $\boldsymbol{x} = (x_1,\ldots,x_d)^T$
- Generate initial n population of sens-objects $\boldsymbol{x}_i = (i = 1, 2,\ldots,n)$
- Find the initial best solution $\boldsymbol{x}^*$ among $\boldsymbol{x}_i$ via $f(\boldsymbol{x}_i)$
- Define a switching probability $\rho \in [0, 1]$
- Define a random number with uniform distribution $\gamma \in [0, 1]$

while ($t <$ MaxMom)
  if ($\gamma > \rho$) % *Population-based*
    - Set $N = n$
    for $i = 1 : N$
      - Generate L by (9) associated with (10) – (13)
      - Create new solution by (8)
    end for
  else if ($\gamma \leq \rho$) % *Single solution-based*
    - Set $N = 1$
    - Generate ε by (15)
    - Create new solution by (14)
  end if
  if $f(\boldsymbol{x}) < f(\boldsymbol{x}^*)$
    - Update current best solution $\boldsymbol{x}^* = \boldsymbol{x}$
  end if
end while
- Report the best solution found

FIGURE 6. Pseudo code of SS algorithm

to create new solutions. Otherwise, ($\gamma \leq \rho$), Rule-2 (single solution-based) is invoked by using the expressions in (14)-(15) to create new solutions. After that, the current best solution will be updated by new solution found. The SS algorithm will be iteratively processed until the optimal solution is found or the termination criteria (TC) are met.

4.2. **PI$^\lambda$D$^\mu$ control loop.** The wind turbine system which is operated under the PI$^\lambda$D$^\mu$ feedback control loop can be represented by the block diagram as shown in Figure 7, where $G_c(s)$ is the PI$^\lambda$D$^\mu$ controller model and $G_p(s)$ is the plant model. Referring to Figure 7, the PI$^\lambda$D$^\mu$ controller receives the error signal, $E(s)$, and produces the control signal, $U(s)$, to control the output response, $C(s)$, referring to the referent input command signal, $R(s)$, and regulate the output response, $C(s)$, from the external load disturbance signal, $D(s)$.

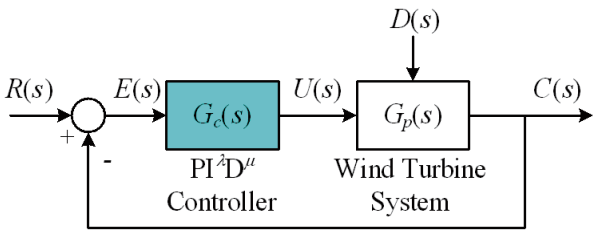

FIGURE 7. PI$^\lambda$D$^\mu$ feedback control loop

4.3. **SS-based PI$^\lambda$D$^\mu$ controller design problem.** The SS-based PI$^\lambda$D$^\mu$ controller design for the wind turbine control system can be represented by the block diagram as shown in Figure 8. The objective function J is performed as the sum-squared error

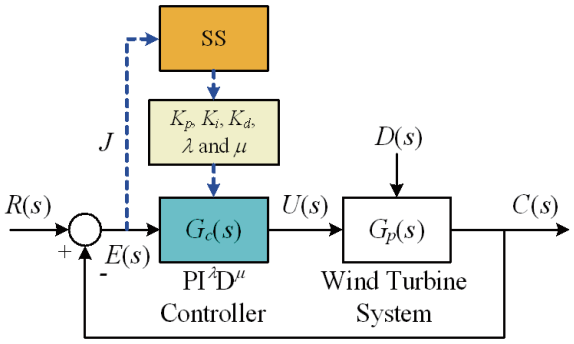

FIGURE 8. SS-based PI$^{\lambda}$D$^{\mu}$ controller design

between the referent input command signal $R(s)$ and the actual output response $C(s)$ as stated in (16). J will be fed to the SS in order to be minimized by searching for the optimal values of K_p, K_i, K_d, λ and μ as the parameters of the PI$^{\lambda}$D$^{\mu}$ controller within their particular boundaries or search spaces as shown in (17).

$$\textbf{Min } J(K_p,\ K_i,\ K_d, \lambda,\ \mu) = \sum_{i=1}^{N} [R_i - C_i]^2 \tag{16}$$

$$\left.\begin{aligned} \textit{Subject to } & t_r \le t_{r\_\max}, \quad M_p \le M_{p\_\max}, \\ & t_s \le t_{s\_\max}, \quad E_{ss} \le E_{ss\_\max}, \\ & K_{p\_\min} \le K_p \le K_{p\_\max}, \\ & K_{i\_\min} \le K_i \le K_{i\_\max}, \\ & K_{d\_\min} \le K_d \le K_{d\_\max}, \\ & \lambda_{\min} \le \lambda \le \lambda_{\max}, \quad \mu_{\min} \le \mu \le \mu_{\max} \end{aligned}\right\} \tag{17}$$

In this work, J will be minimized according to the constrained functions as defined in (17), where t_r and $t_{r\_\max}$ are the rise time and the maximum rise time allowance, M_p and $M_{p\_\max}$ are the percent overshoot and the maximum the percent overshoot allowance, t_s and $t_{s\_\max}$ are the settling time and the maximum settling time allowance, and E_{ss} and $E_{ss\_\max}$ are the steady-state error and the maximum steady-state error allowance, respectively.

When the SS is applied to design the PI$^{\lambda}$D$^{\mu}$ controller for the wind turbine control system, its algorithms can be represented step-by-step to show how the SS finds the optimal parameters K_p, K_i, K_d, λ and μ of the PI$^{\lambda}$D$^{\mu}$ controller as follows.

Step 0 Perform the objective function J as stated in (16) with the inequality constraint functions in (17), the search spaces of K_p, K_i, K_d, λ and μ as in (17), MaxMom (maximum moment of *Citta* or iteration) and Mom = 1 (initialized moment of *Citta*). Initialize the numbers of sens-objects n and a switching probability ρ. In this step, the initial best solutions $\boldsymbol{x}^*$ (initial values of K_p, K_i, K_d, λ and μ) is selected among randomly initial solutions $\boldsymbol{x}_i$ within the given search spaces via the objective function J. A random number with uniform distribution $\gamma \in [0, 1]$ is also defined.

Step 1 If Mon <= MaxMom, uniformly random rand value. Otherwise, go to Step 6.

Step 2 If $\gamma > \rho$, (*Population-based*)
- Set $N = n$.
- Generate L by (9) associated with (10)-(13).
- Create the new solution (K_p, K_i, K_d, λ and μ) by (8).

Otherwise (*Single solution-based*)
- Set $N = 1$.

– Generate ε by (15).
– Create the new solution (K_p, K_i, K_d, λ and μ) by (14).

Step 3 Evaluate new solutions (K_p, K_i, K_d, λ and μ) via the objective function J in (16) associated with the constraint functions in (17).

Step 4 If the J of new solutions is less than the J of old solutions, the solutions $\boldsymbol{x}^*$ (K_p, K_i, K_d, λ and μ) will be updated. Otherwise, the old solutions $\boldsymbol{x}^*$ are maintained.

Step 5 Update Mom = Mom + 1, and go back to Step 1 to proceed the next moment.

Step 6 Terminate the search process and report the best solution (K_p, K_i, K_d, λ and μ).

5. **Results and Discussion.** To design the optimal PI$^\lambda$D$^\mu$ controller of a wind turbine drive train and a pitch control of the wind turbine system, the SS algorithm was coded by MATLAB version 2018b (License No. #40637337). The searching parameters of SS are set according to the recommendations [34] as follows: number of sens-objects $n = 30$ and switching probability $\rho = 0.25$ (or 25%). This searching parameters setting is sufficient for most optimization problems because the SS algorithm is very robust (not very sensitive to the parameter adjustment) [34]. The maximum moment MaxMom = 200 is then set as TC for all cases. 50 trials are conducted to find the optimal PI$^\lambda$D$^\mu$ controllers. For comparison with the PI controller, K_d and μ in (17) will be set as zero and λ in (17) will be set as one. In addition for comparison with the PID controller, μ and λ in (17) will be set as one.

5.1. **Wind turbine drive train control.** For the case of wind turbine drive train control, $G_p(s)$ in Figure 8 will be substituted by $G_{p1}(s)$ in (6). The search spaces and constraint functions in (17) are then performed by preliminary study as given in (18). Once 50 trials of the search process were completed, the SS can successfully provide the optimal PI, PID and PI$^\lambda$D$^\mu$ controllers for the wind turbine drive train control system as shown in (19), (20) and (21), respectively.

$$\left.\begin{array}{l} \textit{Subject to } t_r \le 0.25\text{s}, \quad M_p \le 25\%, \quad t_s \le 2.50\text{s}, \\ \qquad\qquad E_{ss} \le 0.01\%, \quad 0 \le K_p \le 1.0, \quad 0 \le K_i \le 5.0, \\ \qquad\qquad 0 \le K_d \le 0.1, \quad 0.01 \le \lambda \le 1.50, \quad 0.01 \le \mu \le 1.50 \end{array}\right\} \tag{18}$$

$$G_c(s)|_{PI} = 0.5226 + \frac{1.4619}{s} \tag{19}$$

$$G_c(s)|_{PID} = 0.5837 + \frac{3.0111}{s} + 0.0345s \tag{20}$$

$$G_c(s)|_{PI^\lambda D^\mu} = 0.5838 + \frac{3.0112}{s^{1.0310}} + 0.0343s^{1.0512} \tag{21}$$

Figure 9 shows the convergent rates of the objective functions in (16) associated with inequality constraint functions in (17) proceeded by the SS over 50 trials for the PI$^\lambda$D$^\mu$ controller design. It can be observed that the SS has a good robustness for global convergence with different randomly initial solutions. The unit-step command-tracking and the 10%-step load-regulating responses of the wind turbine drive train control system with PI, PID and PI$^\lambda$D$^\mu$ controllers designed by the SS are depicted in Figure 10(a) and Figure 10(b), respectively. All results of this case are summarized in Table 1, where t_{reg} is the regulating time and M_{p_reg} is the maximum percent overshoot of load regulation. From Figure 10 and Table 1, it was found that the PI$^\lambda$D$^\mu$ controller can provide faster and smoother responses than the PI and PID controllers in both command-tracking and load-regulating responses.

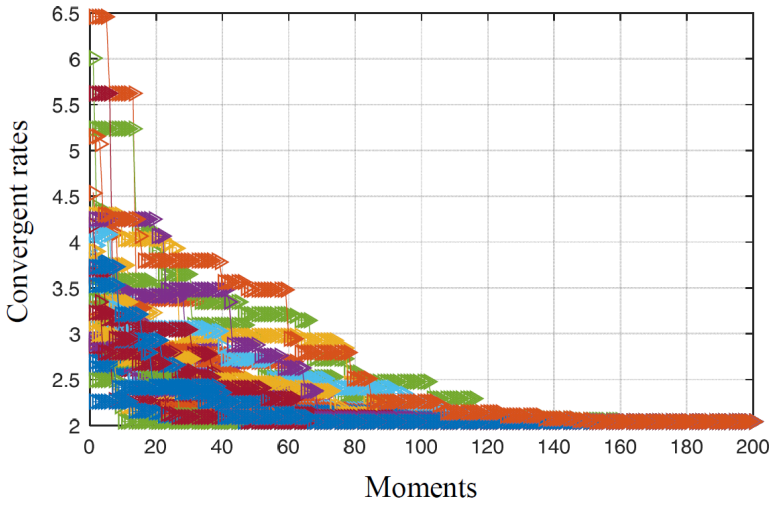

FIGURE 9. Convergent rates of PI$^{\lambda}$D$^{\mu}$ controller designed by SS for drive train control system

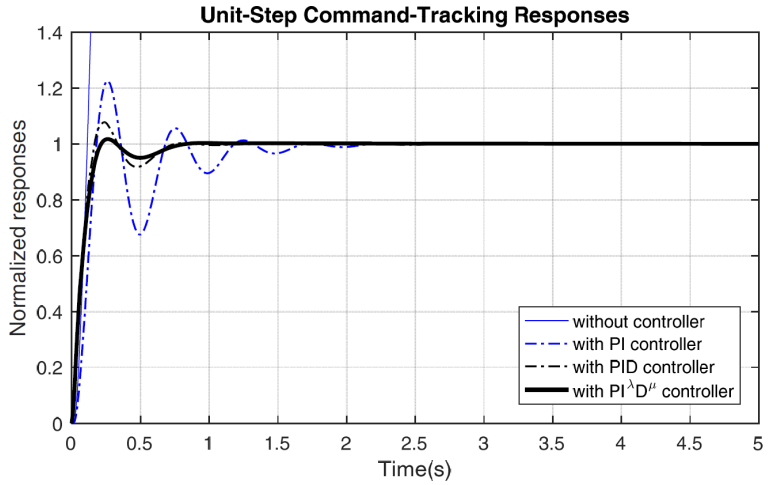

(a)

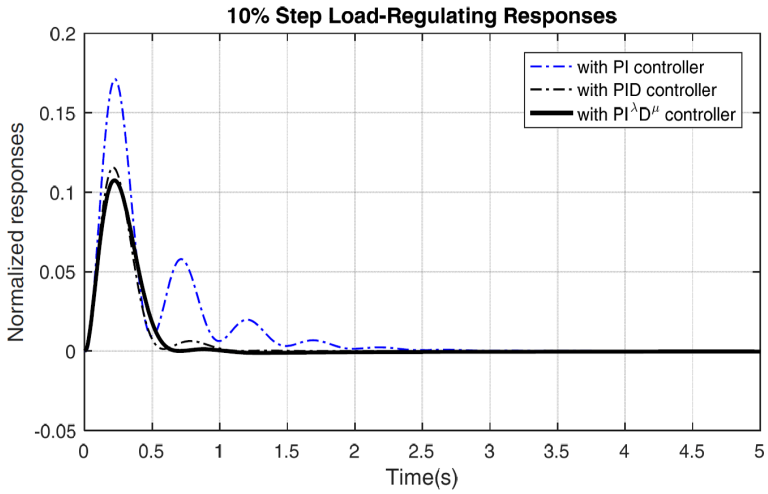

(b)

FIGURE 10. Responses of wind turbine drive train control system: (a) unit-step command-tracking, (b) 10%-step load-regulating

TABLE 1. Results of wind turbine drive train controlled system

Controllers	Unit-step command-tracking responses				10%-step load-regulating responses		
	t_r(s)	M_p(%)	t_s(s)	E_{ss}(%)	t_{reg}(s)	M_{p_reg}(%)	E_{ss}(%)
PI	0.18	22.61	2.18	0.00	2.52	17.12	0.00
PID	0.17	7.78	0.74	0.00	0.87	11.56	0.00
PI$^\lambda$D$^\mu$	0.21	1.73	0.72	0.00	0.69	10.74	0.00

5.2. **Wind turbine pitch control.** For the case of wind turbine pitch control, $G_p(s)$ in Figure 8 will be replaced by $G_{p2}(s)$ in (7). The search spaces and constraint functions in (17) are then performed by preliminary study as given in (22). When 50 trials of the search process were terminated, the SS can successfully provide the optimal PI, PID and PI$^\lambda$D$^\mu$ controllers for the wind turbine pitch control system as shown in (23), (24) and (25), respectively.

$$\left.\begin{array}{l} \textit{Subject to } t_r \le 25.0\text{s}, \quad M_p \le 10\%, \quad t_s \le 30.0\text{s}, \\ \qquad E_{ss} \le 0.01\%, \quad 0 \le K_p \le 2.0, \quad -10.0 \le K_i \le 10.0, \\ \qquad -0.10 \le K_d \le 0.10, \quad 0.01 \le \lambda \le 1.50, \quad 0.01 \le \mu \le 1.50 \end{array}\right\} \tag{22}$$

$$G_c(s)|_{PI} = 0.9868 - \frac{8.5914}{s} \tag{23}$$

$$G_c(s)|_{PID} = 0.9868 - \frac{8.5914}{s} - 0.0275s \tag{24}$$

$$G_c(s)|_{PI^\lambda D^\mu} = 0.9868 - \frac{8.5914}{s^{1.1623}} - 0.0275s^{1.0204} \tag{25}$$

The convergent rates proceeded by the SS for the PI$^\lambda$D$^\mu$ controller design of wind turbine pitch control system are omitted because they have a similar form to that of the turbine drive train control system as shown in Figure 9. The unit-step command-tracking and the unit-step load-regulating responses of the wind turbine pitch control system with PI, PID and PI$^\lambda$D$^\mu$ controllers designed by the SS are plotted in Figure 11(a) and Figure 11(b), respectively. All results of this case are summarized in Table 2. Referring to Figure 11 and Table 2, it was found like a case of drive train control system that the PI$^\lambda$D$^\mu$ controller can provide very satisfactory wind turbine pitch control system responses faster and smoother than the PI and PID controllers in both command-tracking and load-regulating responses.

From the design results of wind turbine drive train and a pitch control of the wind turbine systems, it was found that the SS is very effective for optimizing the PI$^\lambda$D$^\mu$ controller. Moreover, PI$^\lambda$D$^\mu$ controller can yield very satisfactory responses faster and smoother than the PI and PID controllers.

6. **Conclusions.** Designing an optimal PI$^\lambda$D$^\mu$ controller for wind turbine systems using the SS-based on the modern optimization framework has been proposed in this paper. As one of the newest and most efficient hybrid metaheuristic optimization searching algorithms conceptualized by the spiritual concentration according to the Buddhist principles, the SS has been applied to searching for the optimal values of the PI$^\lambda$D$^\mu$ controller parameters within their preset search spaces and constrained functions to achieve both command-tracking and load-regulating purposes. With the proposed SS-based design approach, results obtained by the PI$^\lambda$D$^\mu$ controllers have been compared with those obtained by the PI and PID controllers. The proposed design approach has been demonstrated to design the optimal PI$^\lambda$D$^\mu$ controllers for a drive train and a pitch control of the wind turbine systems. Results obtained from two cases shown that the PI$^\lambda$D$^\mu$ controller designed

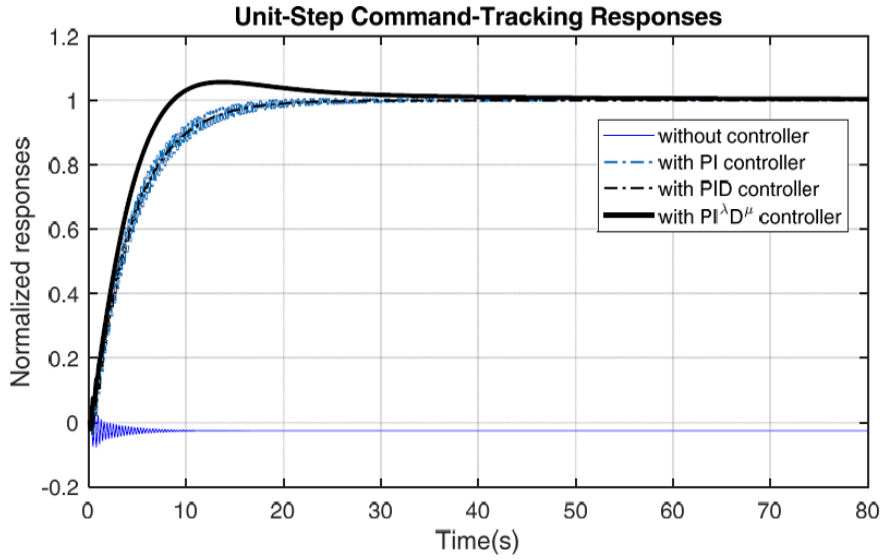

(a)

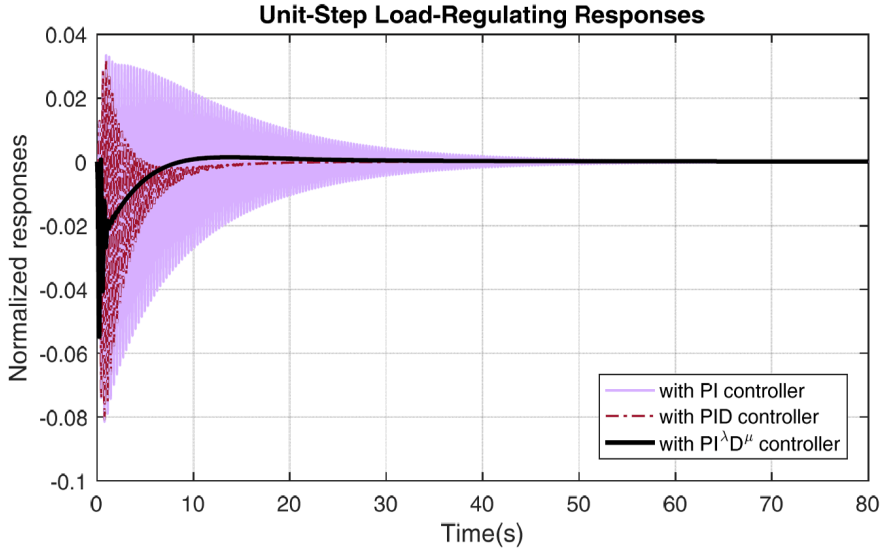

(b)

FIGURE 11. Responses of wind turbine pitch control system: (a) unit-step command-tracking, (b) unit-step load-regulating

TABLE 2. Results of wind turbine pitch controlled system

Controllers	Unit-step command-tracking responses				Unit-step load-regulating responses		
	t_r(s)	M_p(%)	t_s(s)	E_{ss}(%)	t_{reg}(s)	M_{p_reg}(%)	E_{ss}(%)
PI	20.06	0.00	22.14	0.00	46.49	8.15	0.00
PID	20.22	0.00	22.12	0.00	22.14	8.08	0.00
PI$^{\lambda}$D$^{\mu}$	8.64	5.65	28.46	0.00	24.83	5.48	0.00

by the SS could provide faster and smoother responses than the PI and PID controllers in both command-tracking and load-regulating responses. This can be concluded that, with the SS-based design approach, the PI$^{\lambda}$D$^{\mu}$ controller outperforms PI and PID controllers for controlling wind turbine drive train and pitch control systems.

REFERENCES

[1] T. Ackermann, *Wind Power in Power Systems*, John Wiley & Sons, New York, NY, USA, 2005.
[2] D. Chiras, *Wind Power Basics*, New Society Publishers, Canada, 2010.
[3] A. F. Zobaa and R. C. Bansal, *Handbook of Renewable Energy Technology*, World Scientific Publishing Co. Pte. Ltd, 2011.
[4] B. Wu, Y. Lang, N. Zargari and S. Kouro, *Power Conversion and Control of Wind Energy Systems*, John Wiley & Sons, New York, NY, USA, 2011.
[5] S. Behera, B. Subudhi and B. B. Pati, Design of PI controller in pitch control of wind turbine: A comparison of PSO and PS algorithm, *International Journal of Renewable Energy Research*, vol.6, no.1, pp.271-281, 2016.
[6] K. O. Merz, Basic controller tuning for large offshore wind turbines, *Wind Energy Science*, vol.1, pp.153-175, 2016.
[7] S. Baburajan and A. Ismail, Design and control of the pitch of wind turbine through PID, *International Research Journal of Engineering and Technology*, vol.4, no.9, pp.657-661, 2017.
[8] A. Gambier and Y. Y. Nazaruddin, Collective pitch control with active tower damping of a wind turbine by using a nonlinear PID approach, *Proc. of the 3rd IFAC Conference on Advances in Proportional-Integral-Derivative Control*, pp.238-243, 2019.
[9] A. A. Paret, PID controlled frequency regulation of wind turbine, *International Journal of Advanced Research in Electrical, Electronics and Instrumentation Engineering*, vol.3, no.3, pp.7557-7563, 2014.
[10] H. Habibi, H. R. Nohooji and I. Howard, Adaptive PID control of wine turbines for power regulation with unknown control direction and actuator faults, *IEEE Access*, vol.6, pp.37464-37479, 2018.
[11] Y. Qi and Q. Meng, The application of fuzzy PID control in pitch wind turbine, *Energy Procedia*, vol.16, pp.1635-1641, 2012.
[12] O. A. Ahmed and A. A. Ahmed, Control of wind turbine for variable speed based on fuzzy-PID controller, *Journal of Engineering and Computer Sciences*, vol.18, no.1, pp.40-50, 2017.
[13] E. Chavero-Navarrete, M. Trejo-Perea, J. C. Jáuregui-Correa, R. V. Carrillo-Serrano and J. G. Ríos-Moreno, Expert control systems for maximum power point tracking in a wind turbine with PMSG: State of the art, *Applied Sciences*, vol.9, pp.1-24, 2019.
[14] I. Podlubny, *Fractional-Order Systems and Fractional-Order Controllers*, UEF-03-94, Slovak Academy of Sciences, Kosice, 1994.
[15] I. Podlubny, Fractional-order systems and $PI^{\lambda}D^{\mu}$-controllers, *IEEE Trans. Automatic Control*, vol.44, no.1, pp.208-214, 1999.
[16] C. A. Monje, B. M. Vinagre, V. Feliu and Y. Chen, Tuning and auto-tuning of fractional order controllers for industry applications, *Control Engineering Practice*, vol.16, pp.798-812, 2008.
[17] M. Zamani, M. Karimi-Ghartemani, N. Sadati and M. Parniani, Design of a fractional order PID controller for an AVR using particle swarm optimization, *Control Engineering Practice*, vol.17, pp.1380-1387, 2009.
[18] D. Xue, C. Zhao and Y. Q. Chen, Fractional order PID control of a DC-motor with elastic shaft: A case study, *Proc. of the 2006 American Control Conference*, pp.3182-3187, 2006.
[19] A. J. Calderón, B. M. Vinagre and V. Feliu, Fractional order control strategies for power electronic buck converters, *Signal Processing*, vol.86, no.10, pp.2803-2819, 2006.
[20] S. K. Mishra and D. Chandra, Stabilization and tracking control of inverted pendulum using fractional order PID controllers, *Journal of Engineering*, vol.2014, pp.1-9, 2014.
[21] Q. Gao, J. Chen, L. Wang, S. Xu and Y. Hou, Multiobjective optimization design of a fractional order PID controller for a gun control system, *The Scientific World Journal*, vol.2013, pp.1-8, 2013.
[22] D. Valério and J. C. Sáda, Tuning of fractional PID controllers with Ziegler-Nichols type rules, *Signal Processing*, vol.86, no.10, pp.2771-2784, 2006.
[23] Y. Chen, T. Bhaskaran and D. Xue, Practical tuning rule development for fractional order proportional and integral controllers, *Journal of Computational and Nonlinear Dynamics*, vol.3, 2008.
[24] R. Caponetto, L. Fortuna and D. Porto, A new tuning strategy for a non integer order PID controller, *Fractional Differentiation and Its Applications*, Bordeaux, 2004.
[25] C. Zhao, D. Xue and Y. Chen, A fractional order PID tuning algorithm for a class of fractional order plants, *Proc. of the International Conference on Mechatronics & Automation*, Niagara Falls, 2005.
[26] Y. Q. Chen, I. Petráš and X. Dingyü, Fractional order control – A tutorial, *Proc. of the American Control Conference*, pp.1397-1411, 2009.
[27] P. Shah and A. Agashe, Review of fractional PID controller, *Mechatronics*, vol.38, pp.29-41, 2016.
[28] V. Zakian, *Control Systems Design: A New Framework*, Springer-Verlag, 2005.

[29] V. Zakian and U. Al-Naib, Design of dynamical and control systems by the method of inequalities, *Proc. of the IEE International Conference*, vol.120, pp.1421-1427, 1973.
[30] H. M. Hasanien and S. M. Muyeen, Design optimization of controller parameters used in variable speed wind energy conversion system by genetic algorithms, *IEEE Trans. Sustainable Energy*, vol.3, pp.200-208, 2012.
[31] D. C. Das, A. K. Roy and N. Sinha, GA based frequency controller for solar thermal diesel-wind hybrid energy generation/energy storage system, *International Journal of Electrical Power & Energy Systems*, vol.43, pp.262-279, 2012.
[32] I. Poultangari, R. Shahnazi and M. Sheikhan, RBF neural network based PI pitch controller for a class of 5-MW wind turbines using particle swarm optimization algorithm, *ISA Transaction*, vol.51, pp.641-648, 2012.
[33] J. W. Perng, G. Y. Chen and S. C. Hsieh, Optimal PID controller design based on PSO-RBFNN for wind turbine systems, *Energies*, vol.7, pp.191-209, 2014.
[34] D. Puangdownreong, Spiritual search: A novel metaheuristic algorithm for control engineering optimization, *International Review of Automatic Control (IREACO)*, vol.11, no.2, pp.86-97, 2018.
[35] A. Nawikavatan, C. Thammarat and D. Puangdownreong, Application of spiritual search to optimal PIDA controller design for cardiac pacemaker, *Proc. of the 2nd ECTI Northern Section Conference on Electrical, Electronics, Computer and Telecommunications Engineering (ECTI-CON2019)*, pp.286-289, 2019.
[36] C. G. Anderson, J. B. Richon and T. J. Campbell, An aerodynamic moment-controlled surface for gust load alleviation on wind turbine rotors, *IEEE Trans. Control System Technology*, vol.6, pp.577-595, 1998.
[37] J. Wang, N. Tse and Z. Gao, Synthesis on PI-based pitch controller of large wind turbines generator, *Energy Conversion and Management*, vol.52, pp.1288-1294, 2011.
[38] *FAST: An Aeroelastic Computer-Aided Engineering (CAE) Tool for Horizontal Axis Wind Turbines*, http://wind.nrel.gov/designcodes/simulators/fast, accessed on 14 October 2018.
[39] P. Harvey, *An Introduction to Buddhism: Teachings, History and Practices*, Cambridge University Press, 2013.
[40] W. Rahula, *What the Buddha Taught*, Grove Press, New York, 1974.